Magnetic Field Analysis and Measurement of Pulsed Septum Magnet

Jin Tong and Yongfang Liu*

Shanghai Advanced Research Institute
Chinese Academy of Sciences, Shanghai, 201204, China
*liuyongfang@sari.ac.cn

Abstract **–** Traditional off-axis injection becomes inadequate in diffraction limited storage ring (DLSR) for its small dynamic aperture (DA). On-axis injection with thin septum could solve the problem. This paper focuses on the theoretical calculation, field simulation, and measurement of thin septum magnets. The scheme of eddy-current type thin septum magnets (the thinnest portion is with the thickness of 0.9 mm) was adopted with laminated silicon steel sheets as the magnet core. The simulation of main field, stray field along the beam trajectory, the leakage field decayed over 1 millisecond time was carried out within Opera 2D/3D. Field measurement and analysis of thin septum magnets also has been conducted comprehensively. The results meet requirements, and the work laid a foundation for injection technology of an advanced light source.

Index Terms **–** Diffraction limited storage ring (DLSR), eddy current, injection and extraction, magnetic field simulation, septum magnet, thermal analysis.

I. INTRODUCTION

Diffraction limited storage ring (DLSR) injection by traditional off-axis methods is inadequate for its small emittance aperture. Strip-line combined with a Lambertson or thin septum could offer an on-axis injection scheme, as shown in Fig. 1 [1]. This article focuses on the magnetic field simulation, measurement, and analysis of the thin septum. The eddy current type of septum magnet had been adopted for its relatively low power consumption and simple structure [2].

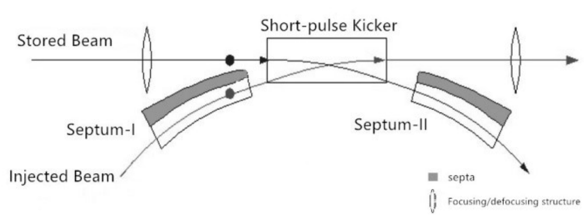

Fig. 1. Diagram of on-axis injection schematic.

II. CALCULATION OF KEY PARAMETERS

The eddy-current type of thin septum magnet is mainly constructed from 4 parts: exciting coil, c-type silicon steel core, septa, and supporting frame. The exciting coil is just one turn oxygen-free copper, which could be led out of the vacuum through feedthrough. The core comprises more than 13,000 lamination silicon steel sheets [3]. The septa part, which is the synthesis of oxygen-free copper and shielding layer, is the most significant assembly unit for the whole septum, and the supporting frame is constructed by oxygen-free copper [4].

$$I_p = B*(G_m + {}^{l_c}/_{u})/(u_0 * N). \quad (1)$$

In equation (1), G_m is the magnet gap height, which is 12 mm and l_c is the length of core path, which is approximately 150 mm. Besides, N indicates the number of turns on magnet. The peak of exciting current is 5322 A.

$$L=\mu_0 * A_m * \mathrm{w_m} * N^2/(G_m + {}^{l_c}/_{u}). \quad (2)$$

Similarly, A_m and W_m represent the magnet gap width 40 mm and the magnet gap height 12 mm respectively. The equivalent inductance of the septum magnet is 2.5 μH.

According to the requirements of physical design, key parameters of the thin septum may be seen in Table 1.

Table 1: Key parameters of the eddy-current septum

Parameters	Value	Unit
Beam energy	2	GeV
Deflection angle	50	mrad
Integral field	0.32	T*m
Peak field	5560	Gauss
Good field region	28*10	mm*mm
Mini. septum Thickness	0.9	mm
Peak current	5322	A
Magnet inductance	2.5	μH
Leakage field	0.1%	–

Submitted On: February 26, 2023
Accepted On: November 22, 2023
https://doi.org/10.13052/2023.ACES.J.380917

III. MODELING ANALYSIS

A. 2D transient optimization

According to the magnet size setting, two-dimensional static analysis could be conducted in OPERA finite element analysis software by modeling the magnet with clear boundary conditions. Specific analysis shows that the magnetic field between the center of the magnetic gap is approximately 5600 gauss.

The basic operation principle of thin septum is that the pulsed magnetic field could induct eddy current on oxygen-free copper septa, which could generate a field to effectively offset the leakage part instantly. High-permeability materials could deal with almost all of the remaining overflow magnetic field.

Figure 2 shows some dynamic analysis results. Transverse homogeneity of the main field in central area is$\pm$0.45%, and the leakage field under different thicknesses of septa, which was decaying over 1 ms, was thoroughly recorded.

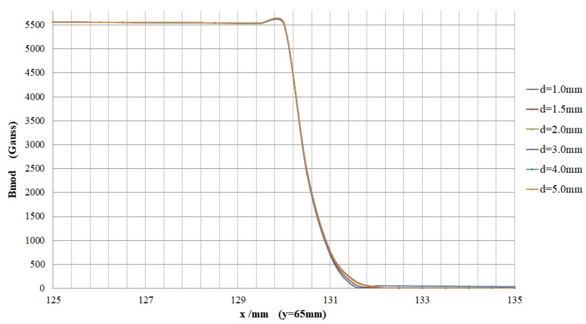

Fig. 2. Leakage magnet field with different septa.

B. 3D transient analysis

The key point of 3D transient analysis of the thin eddy-current septum with OPERA lies in the technique of 3D mesh generation [5]. Poor meshing could lead to misconvergence output. In this project, the mechanical length of the magnet is 660 mm, and the length of the silicon steel core (laminated coefficient is 0.98) is 600 mm. Meanwhile, the thickness of the septa is as thin as 0.9 mm (0.6 mm oxygen-free copper plus 0.3 mm shield layer). In order to achieve a balance between precision outcomes and appropriate computational volume, the ratio between the small-scale grids of the key parts and the large scale grids of other parts should not be too disparate during the process of meshing (Fig. 3). The maximum angle between elements and maximum deviation from surface were set as 90°and 0.2 mm. The maximum element sizes are 1 mm, 0.8 mm, 0.5 mm, and 0.3 mm for the silicon steel core, oxygen-free copper framework, oxygen-free copper septa, and the shield layer, respectively. Finally, more than a million regular tetrahedrons

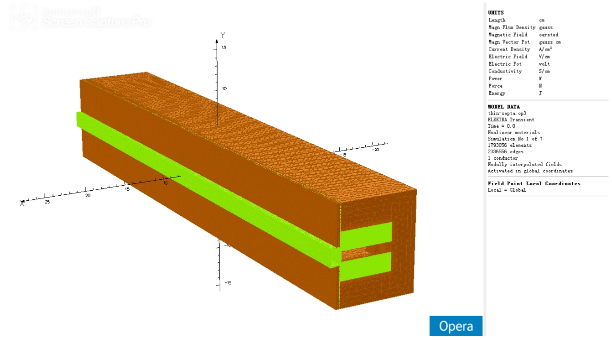

Fig. 3. 3D model of the thin septum magnet.

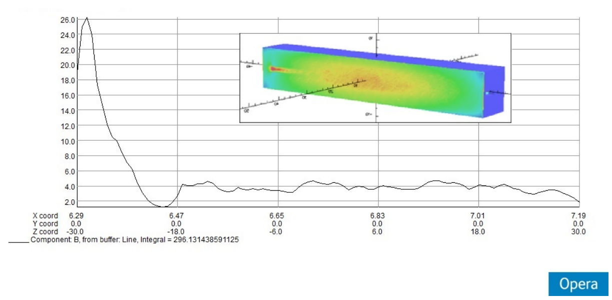

Fig. 4. Results of three dimensional analysis.

had been divided with the opera-3D modeler. The simulation was conducted on an Intel(R) Core^{TM} i5@3.2 GHz, 4GB RAM desktop computer and took almost 30 hours for the result.

The line integrals of the main magnetic field and the leakage field along the beam direction, just 2 mm away from the septa, are shown in Fig. 4. The final result after the ends shielding optimization is 0.09%, which could satisfy the requirement of 0.1%.

Furthermore, the dynamic analysis of the single thin sheet silicon steel of the magnet septum was conducted, and the distribution of induced current could be clearly seen, as shown in Fig. 5.

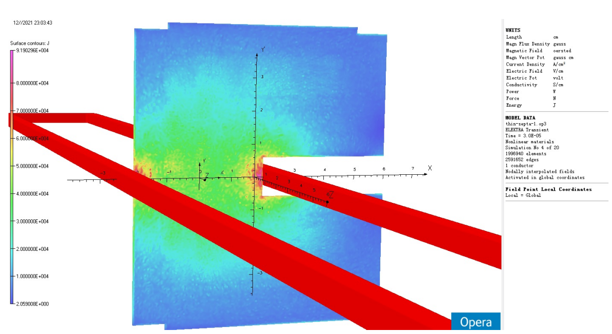

Fig. 5. Eddy current on single slice of silicon steel.

C. Thermal analysis

Because the eddy current septum is designed as an in-vacuum magnet, special attention should be paid to its own heating power consumption and temperature distribution. Heat conduction analysis of the septum magnet should be conducted strictly.

According to the basic theory of steady-state heat conduction [6], The temperature gradient $grad(t)$ is defined as the limit of the temperature increment Δt and the ratio of the normal distance Δn along the isothermal surface,

$$grad(t) = \lim_{\Delta n \to 0} \frac{\Delta t}{\Delta n} = \frac{\partial t}{\partial n} \vec{n}. \tag{3}$$

The heat flux $\vec{q}$ is proportional to the temperature gradient grad.

$$\vec{q} = -\lambda \mathrm{grad}(t) = -\lambda \frac{\partial t}{\partial n} \vec{n} \tag{4}$$

where λ is the thermal conductivity of W/(mK).

According to the analysis, the sources of heating for the septum are copper exciting coil, laminated silicon steels, and oxygen free copper septa. After setting the thermal conductivity of related materials (see Table 2), the steady-state thermal analysis was carried out.

Table 2: Thermal conductivity of septum components

	Material	Thermal conductivity
Coil	Ox- free copper	387.6 W/(m·K)
Insulating	Polyphenylene sulfide	0.28 W/(m·K)
Core	Non-oriented silicon steel	0.3 W/(m·K)
Septa	Ox- free copper	387.6 W/(m·K)
Shielding	Oriented silicon steel	0.3 W/(m·K)
Frame	Ox-free copper	387.6 W/(m·K)

The initial temperature of all the components is 24 degrees Celsius . According to the power density results at 0.5 Hz repetition rate, the highest temperature of the whole magnet is about 28°C (Fig. 6).

Figure 7 shows the temperature distribution on the outer surface of the septa plate with eddy current septum, which is 1∼2°C higher than the base temperature. Therefore, the excitation heating problem is not serious, hence no need for water cooling and other special measures. The magnet base and stainless steel adjustment platform could conduct the heat to the outside of the vacuum box for heat dissipation.

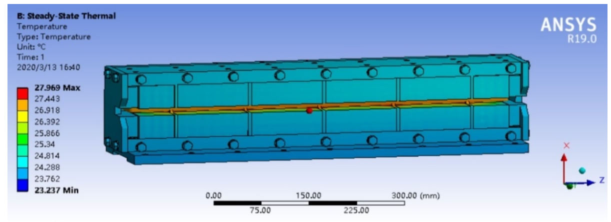

Fig. 6. Internal temperature distribution of the septum.

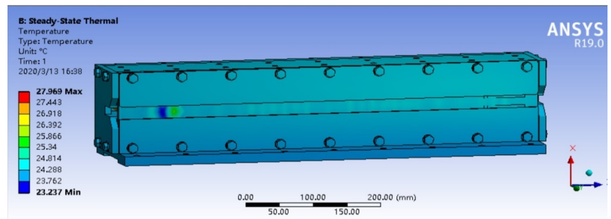

Fig. 7. Temperature distribution of the septa.

IV. Magnetic field measurement and analysis

After the thin septum magnet was assembled, the capacitor charging and LC resonance discharge pulse power (Fig. 8), which can output a stable peak of 5500 A with bottom width of 50 µS half-sine wave, could be used to energize the magnet coil. The convenient and accurate magnetic field measurement platform was built for the analysis of magnetic field data related to the septum magnet, too (Fig. 9). The automatic magnetic measurement system, using carbon fiber to carry the magnetic coil, works effectively in the lab.

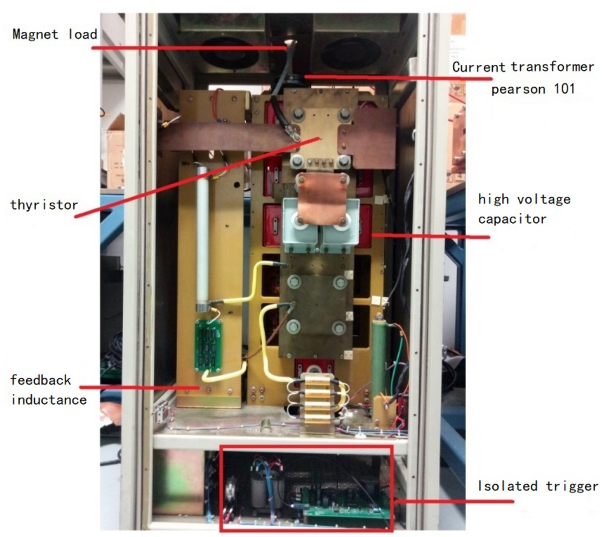

Fig. 8. Layout of excitation pulse power supply.

Fig. 9. Point coil for measuring the end field.

Figure 10 shows the measurement of distribution of the main magnetic field along the beam direction using a point coil with a diameter of 4 mm and 20 turns. Due to the limitation of the length of the measurement probe, only half of the length of the magnet has been tested. The other half of the magnetic field can be measured in the same way. The accuracy of the 12-bit oscilloscope HDO 4104 with digital integrator is so high that the magnetic field test accuracy of half-length magnet is mainly determined by the position accuracy of the moving platform, and the position accuracy is 0.1 millimeter. The other half of the field is measured by rotating the magnet and then testing.

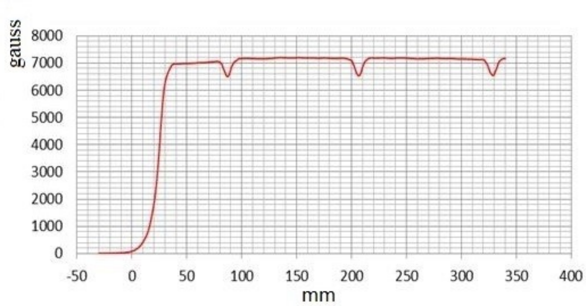

Fig. 10. Field distribution along beam direction.

Furthermore, the point coil (20 turns of φ4 mm) can be used to test the data related to the magnet end field, including the spatial distribution of the end field (Fig. 11) and the decay of the leakage field outside the septa within time and space (Fig. 12) [7]. The *y*-axis in Fig. 12 represents the spatial distribution of the leakage magnetic field at the end region of the septum with 0,1 to 10.13 mm away from the septa .

In Fig. 13, the red waveform shows the excitation current, which reaches 6000A at the peak. The green waveform shows the induced voltage, which is mixed with a certain amount of interference. Finally, the yellow waveform shows the integral of the induced voltage, which is equal to leakage field.

Using the same long coil with a width of 6 mm and a length of 900 mm, the integral value of the main magnetic field against time and the integral value of the leakage magnetic field against time at 3 mm outside the septa have been tested: 2.5 mVs and 1.985 μVs, respectively. The integral ratio of the leakage against the main magnetic field is estimated to be 0.079%, better than the technical requirement of 0.1%.

Finally, the measured temperature distribution is in good agreement with the theoretical calculation. as shown in Fig. 14.

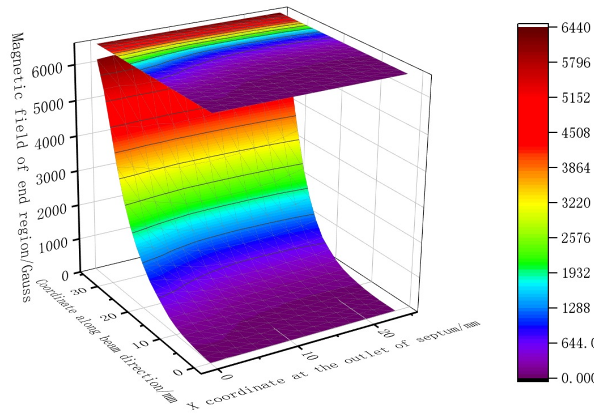

Fig. 11. Color diagram of end field distribution.

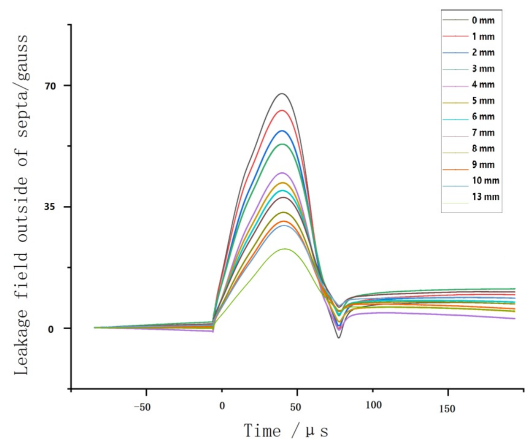

Fig. 12. Leakage field varying with time and space.

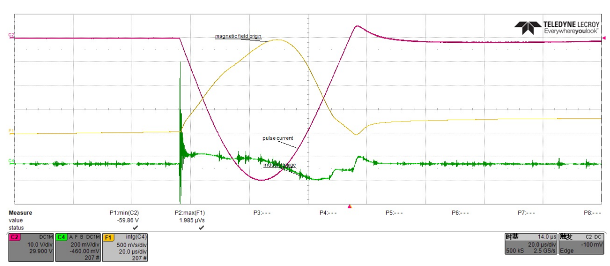

Fig. 13. Induced voltage and integration of leakage field.

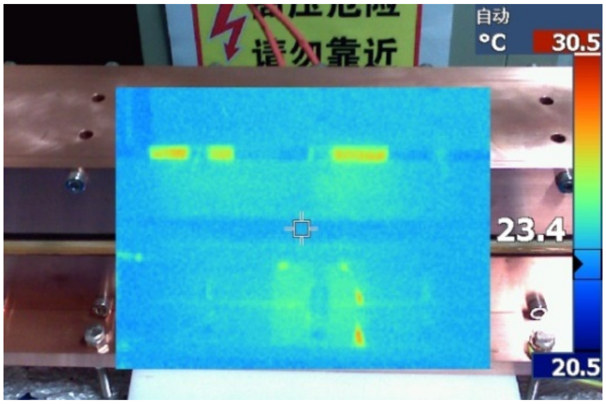

Fig. 14. Temperature distribution at 0.5Hz.

V. CONCLUSION

This paper aims at 3D transient analysis and processing optimization of the thin eddy-current septum for beam injection of a diffraction limited storage ring, especially about simulation and field measurement analysis of the septa. The magnetic excitation power source and the magnetic measurement platform had also been conducted. The results show that the key performance measures of the magnet could all meet the requirements. Furthermore, the theoretical calculations are in good agreement with the measured data in terms of magnetic field and temperature distribution. The work lays a foundation for the next generation of light-source injection technology.

ACKNOWLEDGMENT

Project supported by the National Natural Science Foundation of China (No.12005282) and Youth Innovation Promotion Association of Chinese Academy of Sciences (No. 2021283).

REFERENCES

[1] C. Swenson, D. Arbelaez, J.-Y. Jung, J. Osborn, S. Prestemon, E. Wallen, R. Schlueter, C. Steier, C. Sun, and D. Robin, "Conceptual design of storage ring magnets for a diffraction limited light source upgrade of ALS, ALS-U," in *Proceedings of IPAC2016, Busan, Korea*, pp. 1161-1163, May 2016.

[2] L. H. Ouyang, M. Gu, B. Liu, and R. Chen, "Eddy current septum magnets for injection and extraction at SSRF," *Chinese Physics C*, vol. 34, no. 3, pp. 389-39, 2010.

[3] W. Kang, X. P. Deng, Q. Han, J. B. Pan, and S. Y. Chen, "Theoretical analysis and computer simulation of eddy-current septum magnets," *High Energy Physics and Nuclear Physics*, vol. 25, no. 3, pp. 264-270, 2011.

[4] C. Y. Kuo, C. S. Yang, F. Y. Lin, and Y. L. Chu, "Design and measurement of the septum magnet for the Taiwan Photon Source," *IEEE Transactions on Applied Superconductivity*, vol. 22, no. 3, 4101704, 2012.

[5] F. Zhang, X. Yan, X. Zhang, and F. Wang, "Numerical analysis of magnetic field measurement based on Faraday rotation in a no-core tellurite fiber," *Optical Fiber Technology*, vol. 63, 2021.

[6] L. Christensen, R. Celestina, S. Sperling, R. Mathison, H. Aksoy, and J. Liu, "Infrared temperature measurements of the blade tip for a turbine operating at corrected engine conditions," *Journal of Turbomachinery*, pp. 1-35, 2021.

[7] A. A. Kirilenko, D. Y. Kulik, L. A. Rud, V. I. Tkachenko, and N. Herscovici, "Electromagnetic modeling and design of dual-band septum polarizers, *Applied Computational Electromagnetics Society (ACES) Journal*, vol. 21, no. 2, pp. 155-163, 2022.

Jin Tong graduated from the University of Chinese Academy of Sciences, majoring in nuclear technology and application. Since graduation, he has been engaged in the design of pulse magnets and magnetic measurement systems over years, especially for special magnets used in electron beam injection and extraction systems, such as linear/nonlinear kicker magnets, eddy current septum magnets and Lambertson cutting magnets, which had been designed and researched in large scientific facilities.

Yongfang Liu received the Ph.D. degree in Shanghai Institute of Applied Physics (SINAP) from the University of Chinese Academy of Sciences (UCAS), Beijing, China, in 2020. He is a member of the Shanghai Synchrotron Radiation Facility in Shanghai Advanced Research Institute, Chinese Academy of Sciences. His research interest includes pulsed power and pulsed magnet technologies, such as pulsed klystron modulators, linear transformer drivers (LTD), accelerator pulsed magnets, and power supply.